

Development of Novel Radiotracer for Imaging High Affinity Choline Transporter and Vesicular and Acetyl Choline Transporter

メタデータ	言語: eng 出版者: 公開日: 2017-10-05 キーワード (Ja): キーワード (En): 作成者: メールアドレス: 所属:
URL	http://hdl.handle.net/2297/40326

This work is licensed under a Creative Commons Attribution-NonCommercial-ShareAlike 3.0 International License.



Doctoral Dissertation

Development of Novel Radiotracer for Imaging High Affinity
Choline Transporter and Vesicular Acetyl Choline Transporter

Graduate School of Natural Science & Technology, Kanazawa University.

Division of Life Science

&

Central Institute of Radioisotope Science, Division of tracer kinetics,

Advanced Science Research Center, Kanazawa University.

Major Subject: Division of Life Sciences

Course: Molecular Effects

School Registration No.: 1123032330

Name: Azim Mohammad Anwar-UI

ABSTRACT

Deficiency in HAcHt and VAcHt are characteristic neurochemical changes in AD. The purpose of the dissertation was to evaluate THA derivatives as HAcHt imaging probe and also to develop a radiolabeled decalinvesamicol analogue as a PET VAcHt imaging probe. *In vitro* [³H]HC-3 binding assay of THA, DMTA, PTAA, and MKC-231 revealed no affinity for HAcHt. To develop as VAcHt PET ligand, [⁷⁷Br]OBDV was radiosynthesized with a radiochemical yield of 52.3-65.8% and radiochemical purity of > 99%. The specific activity of [⁷⁷Br]OBDV was found 322 ~ 405.7 GBq/μmol. In *in vivo* biodistribution studies, at 30 min post-injection, the average accumulation of [⁷⁷Br]OBDV in cortex, striatum and cerebellum of rat's brain was 0.52 ± 0.11% ID/g, 0.59 ± 0.05% ID/g and 0.56 ± 0.04% ID/g respectively. In *in vivo* blocking studies, (+/-)-vesamicol blocked regional brain uptake of [⁷⁷Br]OBDV by 41%. In contrast, no blocking effects were observed by both the (+)-3-PPP and (+)-pentazocine. In *ex vivo* autoradiography, accumulation of [⁷⁷Br]OBDV was observed in VAcHt rich brain regions. Hence, OBDV labeled with ⁷⁶Br was suggested to be a potent PET VAcHt imaging probe.

Key words: VAcHt, HAcHt, PET Ligand, AD disease, THA, HC-3, Decalinvesamicol.

Introduction:

Alzheimer's disease (AD) is the most common form of irreversible dementia and characterized clinically by progressive deterioration of intellectual abilities, including cognitive and behavioral dysfunctions. The degeneration of cholinergic neurons in the basal forebrain and the associated loss of the cholinergic neurotransmission in the cerebral cortex and other area contributed significantly to the deterioration in cognitive function in AD. Deficiency in high affinity choline uptake (HACU) and the loss of vesicular acetylcholine transporter (VACHT), are two characteristic neurochemical changes in AD. The HACU by HACHT in peripheral and central cholinergic nerve terminals plays a regulating and rate-limiting role in the intraneuronal synthesis of acetylcholine (ACh). The transportation of newly synthesized ACh the cholinergic synaptic vesicles is mediated by VACHT. Hence, radioligands which bind specifically to the HACHT or VACHT, are assumed to be used as a neuroimaging probe to investigate the cholinergic neurodegenerative process using PET or SPECT.

Objectives:

One of the objective of the dissertation was to evaluate MKC-231, tacirine (THA), and it's corresponding 2-oxo-1-pyrrolidineacetyl derivative as HACHT imaging probe and also to find out the possible explanation of mode of action of HACU enhancer. For this reason we have synthesized THA, DMTA (2,3-dimethylfuran derivative of THA) and their corresponding 2-oxo-1-pyrrolidineacetyl derivatives, namely PTAA and MKC-231 (Fig. 1) and evaluated the affinity of these synthesized compounds for HACHT through *in vitro* [³H]hemicholinium-3 ([³H]HC-3) HACHT binding assay.

In 2012, Kozaka T et al., synthesized two new decalinvesamicol (DV) analogues, *o*-bromo-*trans*-decalinvesamicol (OBDV) and *o*-iodo-*trans*-decalinvesamicol (OIDV) and OBDV was found to possess higher affinity than OIDV towards VACHT and also higher

selectivity over sigma receptors (Table 1). Considering the benefits of using long-lived PET radioisotopes as imaging probe and also considering the *ortho* position of –Br substituent in OBDV, the another objective of the PhD thesis is to develop a radiobromine labelled OBDV (Fig. 2) as a PET radioligand.

The dissertation can be divided in to two parts. Part A includes evaluation of tacirine derivatives as HACHT imaging probe and Part B involves the evaluation of radiobromine labeled OBDV as PET VACHT imaging probe.

PART A: Evaluation of tacirine derivatives as HACHT Imaging probe.

1 Results:

1.1 Chemistry:

The cyclization of 2-Amino benzonitrile (**1**) and 2-Amino-4,5-dimethyl-3-furancarbonitrile (**2**) with cyclohexanone by means of ZnCl₂ in toluene, furnished THA (**3**) and DMTA (**4**), respectively (Fig. 3). The acylation of THA (**3**) and DMTA (**4**) with methyl 2-oxo-1-pyrrolidineacetate furnished PTAA (**5**) and MKC-231 (**6**) with the yield of 79% and 65% respectively (Fig. 4).

1.2 *In vitro* HACHT [³H]HC-3 binding assay:

The inhibition activities of THA, MKC-231 and the two newly synthesized tacirine derivatives, namely DMTA and PTAA were measured by displacement of a typical HACHT antagonist [³H]HC-3 ($K_d = 19.1$ nM) (Quirion R., 1987) in rats cerebral membrane. The percent inhibition against the binding of [³H]HC-3 to HACHT were calculated using GraphPad Prism v4 software (Figure 5).

2 Discussions:

HC-3 is an indirect acetylcholine antagonist, because it decreases the synthesis of acetylcholine by inhibiting the reuptake of choline by the HACHT. HC-3 showed the highest affinity for HACHT ($IC_{50} = 20$ nM). THA showed very insignificant inhibition

activity ($IC_{50} = 1000$ nM). DMTA and PTAA showed no affinity for HACHT. Though MKC-231 is known to enhance HACU, it also did not show any affinity for the HACHT. Other inhibitors like choline chloride (ChCl), Acetylcholine chloride (AChCl), Carbamylcholine Chloride (CaChCl) showed no binding affinity for HACHT.

3. Experimental

3.1 Synthesis of tacirine (3)

To a mixture of 2-Aminobenzonitrile (**1**) (2 g; 16.93 mmol) and cyclohexanone (14 mL; 135.44 mmol) in toluene (60 mL) placed in a round bottom flask connected to a Dean-Stark water separator, $ZnCl_2$ (6.93 g; 50.79 mmol) was added. The mixture was refluxed for 06 hours. After that, the reaction mixture was cooled at room temperature and the remaining solids were treated with NaOH (2M, 70 mL). This mixture was then again refluxed for about another 06 hours with stirring. On cooling to room temperature, the reaction mixture were extracted with $CHCl_3$. The organic layers were combined, dried over anhydrous $MgSO_4$ and concentrated to dryness under reduced pressure. Purification of the residue by column chromatography on silica-gel by using ethyl acetate with trace Et_3N afforded the target compound (**3**) (3.10 g, 92.26 %) as a yellow solid; 1H NMR δ 7.90-7.87 (d, 1H), 7.70-7.67 (d, 1H), 7.58-7.54 (t, 1H), 7.38-7.34 (t, 1H), 4.63 (s, 2H), 3.05-3.01 (t, 2H), 2.64-2.60 (t, 2H), 1.98-1.90 (m, 4H); ^{13}C NMR δ 158.60, 146.58, 146.24, 128.92, 128.40, 123.85, 119.50, 117.13, 110.44, 34.14, 23.75, 22.86, 22.78. EI MS m/z 199 (M^+ , 86.2).

3.2 Synthesis of DMTA (4):

To a mixture of 2-Amino-4,5-dimethyl-3-furancarbonitrile (**2**) (2.00 g; 14.69 mmol) and cyclohexanone (12 mL; 117 mmol) in toluene (60 mL) placed in a round bottom flask connected to a Dean-Stark water separator, $ZnCl_2$ (6 g; 44.00 mmol) was added. The mixture was refluxed for 06 hours. After that, the reaction mixture was cooled at room

temperature and the remaining solids were treated with NaOH (2M, 70 mL). This mixture was then again refluxed for about another 06 hours with stirring. On cooling to room temperature, the reaction mixture were extracted with CHCl₃. The organic layers were combined, dried over anhydrous MgSO₄ and concentrated to dryness under reduced pressure. Purification of the residue by column chromatography on silica-gel by using hexane: ethyl acetate (1:1) with trace Et₃N afforded the target compound (**4**) (1.37 g, 43.08 %) as a yellow solid; ¹H NMR δ 4.35-4.30 (s, 2H), 2.89-2.85 (t, 2H), 2.47-2.45 (t, 2H), 2.30 (s, 6H), 1.91-1.81 (m, 4H); ¹³C NMR δ 160.42, 151.34, 146.10, 145.67, 110.24, 107.28, 105.22, 33.04, 29.00, 22.94, 22.89, 11.28, 10.27. EI MS *m/z* 217 (M⁺, 86.9).

3.3 Synthesis of PTAA (**5**).

To a mixture of tacirine (**3**) (1 g; 5.04 mmol) and DMF (50.4 mL), NaH (4.032 g; 100.08 mmol) was added at room temperature maintaining Argon environment. After 01 hour of stirring, methyl 2-oxo-1-pyrrolidineacetate (2.03 mL; 15.12 mmol) was added to the reaction mixture maintaining the argon environment at room temperature. The reaction was kept in stirring for another one hour at room temperature. After a total of 2 hour, the reaction mixture were extracted with ethyl acetate. The organic layers were combined, dried over anhydrous MgSO₄ and concentrated to dryness under reduced pressure. Purification of the residue by column chromatography on silica-gel by using ethyl acetate: ethanol (50:1) with trace Et₃N afforded the target compound (**5**) (1.3 g, 79.75 %); ¹H NMR δ 8.57-8.56 (s, 1H), 7.99-7.96 (d, 1H), 7.76-7.72 (d, 1H), 7.64-7.59 (t, 1H), 7.48-7.43 (t, 1H), 4.22 (s, 2H), 3.68-3.63 (t, 2H), 3.15-3.10 (t, 2H), 2.80-2.75 (t, 2H), 2.50-2.44 (t, 2H), 2.17-2.10 (m, 2H), 1.98-1.93 (m, 2H), 1.88-1.82 (m, 2H); ¹³C NMR δ 176.76, 166.99, 159.85, 146.90, 137.75, 128.83, 127.22, 126.06, 123.55, 121.95, 49.01, 48.24, 33.99, 30.38, 25.54, 22.67, 22.45, 18.25. EI MS *m/z* 324 (M⁺, 78.6).

3.4 Synthesis of MKC-231 (6).

To a mixture of DMTA (4) (0.338 g; 1.56 mmol) and DMF (15.6 mL), NaH (1.248 g; 31.2 mmol) was added at room temperature maintaining Argon environment. After 01 hour of stirring methyl 2-oxo-1-pyrrolidineacetate (0.63 mL; 4.63 mmol) was added to the reaction mixture maintaining the argon environment at room temperature. The reaction was kept in stirring for another one hour at room temperature. After a total of 2 hour, the reaction mixture were extracted with ethyl acetate. The organic layers were combined, dried over anhydrous MgSO₄ and concentrated to dryness under reduced pressure. Purification of the residue by column chromatography on silica-gel by using ethyl acetate with trace Et₃N afforded the target compound (6) (0.350 g, 65%); ¹H NMR δ 8.45 (s, 1H), 4.14 (s, 2H), 3.64-3.59 (t, 2H), 2.96-2.91(t, 2H), 2.64-2.59 (t, 2H), 2.47-43 8t, 2H), 2.32-2.09 (m, 8H), 1.88-1.76 (m, 4H); ¹³C NMR δ 176.48, 167.67, 159.95, 151.65, 150.14, 134.91, 123.50, 116.37, 108.19, 48.84, 47.71, 32.74, 30.29, 24.25, 22.69, 22.60, 18.12, 11.58, 8.92. EI MS *m/z* 342 (M⁺, 81.4).

4 Preparation of rat cerebral and liver membranes:

Animal experiments were performed in compliance with the *Guidelines for the Care and Use of Laboratory Animals* at the Takara-machi Campus of Kanazawa University. Brain Homogenate of rats were prepared with the slight modification of previously described protocol of Sandberg K et al, 1985. Sprague-Dawley (SD) rats (8 weeks, male, 250–300 g) cerebrum or livers were homogenized in ice-cold 0.32 M sucrose with a Teflon-glass homogenizer. The homogenate was centrifuged at 1000 × g at 4 °C for 10 min. The resulting precipitate was removed and the supernatant was centrifuged at 20,000 × g at 4 °C for 20 min. This crude mitochondrial pellet was resuspended in 20 vols. of ice-cold distilled water and dispersed with the Teflon homogenizer with 1000 rpm and the homogenate centrifuged at 8000 × g run for 20 min. The supernatant and buffy coat were

collected and pelleted at $48,000 \times g$ for 20 min. The pellet was washed 4 times in 20 vols. of 50 mM Glycylglycine buffer (pH 7.8) containing 200 mM NaCl by resuspending via Teflon homogenizer. Then the homogenate was centrifuged at $55,000 \times g$ for about 15 min and the resulting pellet was again resuspended in 50 mM Glycylglycine buffer (pH 7.8) containing 200 mM NaCl with a Teflon homogenizer.

5 *In vitro* HAChT [³H]HC-3 binding assay:

[³H]Hemicholinium-3 ($K_d = 19.1$ nM) (Quirion R 1987) was used as a specific radioligand for the HAChT receptor. Rat cerebral membranes were added to each ice-cold assay tube containing [³H]HC-3 and the displacing ligands at various concentrations ($1.0 \times 10^{-9} - 10^{-4}$) in 50 mM Glycylglycine buffer (pH 7.8) containing 200 mM NaCl in quadruplicate. After the addition of tissues in an ice bath, each reaction mixture in the tube was incubated at 25°C for 30 min. The incubation was terminated by pitting tubes into ice-cold water followed by immediate filtration using a cell harvester through glass-microfiber filters (Whatman, GF/B), which were presoaked in the in 0.5% (v/v) polyethyleneimine for 01 h to reduce non-specific binding. The filters were washed with 50 mM Tris-HCl buffer (pH 7.8), and their radioactivities were counted with the liquid scintillation counter (Aloka, LSC-5100).

PART B: Evaluation of radiobromine labeled decalinvesamicol derivative as VAChT Imaging probe.

1. Results:

1.1 Chemistry: Synthesis of OBDV and OTDV

4-(2-bromophenyl) piperidine (**7**), the key intermediate for the synthesis of OBDV, was derived from *ortho*-bromobenzaldehyde by four-step reactions (Figure 6) (Kozaka T et al., 2012). Coupling reaction of 4-(2-bromophenyl) piperidine with *trans*-decalin-2,3-oxide furnished OBDV(**8**) in 57% yield. The bromo substituent of OBDV was replaced by

a trimethylstannyl group with the reaction of Pd(PPh₃)₄ and hexamethylditin to obtain the corresponding precursor, *o*-trimethylstannyl-*trans*-decalinvesamicol (OTDV) (**9**), for the radiosynthesis of [⁷⁷Br]OBDV, with an yield of 65%

1.2 Radiosynthesis and purification of [⁷⁷Br]OBDV:

[⁷⁷Br]OBDV was radiosynthesized with a radiochemical yield of 52.3-65.8%. [⁷⁷Br]OBDV was purified with reversed phase HPLC equipped with a Zorbax-ODS RX-C18 column (9.6 mm × 250 mm) at a flow rate of 4.0 mL/min with a mobile phase of acetonitrile: H₂O: monoethanolamine (90:10:0.2, v/v/v) at 40°C and radiochemical purity was found to be greater than 99%. Ultraviolet (UV) absorption was monitored at 230 nm. The retention time of [⁷⁷Br]OBDV was found 10 min (Figure 8). The specific activity of [⁷⁷Br]OBDV prepared by the tin-bromine exchange reaction was found to be 322 ~ 406 GBq/μmol (9.8 ~ 10.9 Ci/μmol).

1.3 *In vivo* biodistribution of [⁷⁷Br]OBDV:

At 30 and 60 min post-injection, the average accumulation of [⁷⁷Br]OBDV in all brain regions of interest was 0.56 ± 0.06% ID/g and 0.50 ± 0.05% ID/g, respectively (Table 2). Blood clearance of [⁷⁷Br]OBDV was also very rapid and at 2 min post-injection, the radioactivity in blood was 0.14 ± 0.01% ID/g. High radioactivity was observed in the pancreas (2.98 ± 0.33% ID/g) and small intestine (1.69 ± 0.26% ID/g) with maximum accumulation 60 min after injection. At 2 min post-injection, the accumulation of radioactivity in the lung was very high (5.57 ± 0.72% ID/g), but the radioactivity decreased to 1.23 ± 0.14% ID/g 60 min after injection.

1.4 *In vivo* blocking studies

With co-administration of 0.250 μmol (+/-)-vesamicol, uptake of [⁷⁷Br]OBDV in the cerebral cortex, striatum, cerebellum, and the rest decreased to 42%, 43%, 42%, and 45%, respectively, relative to the control (Figure 9). Tukey's multiple comparison test in

conjunction with an ANOVA revealed very significant ($P < 0.001$ to $P < 0.01$) inhibition effect of (+/-)-vesamicol on the uptake of [^{77}Br]OBDV in all brain regions. However, with co-administration of (+)-pentazocine or (+)-3-PPP, the accumulation of [^{77}Br]OBDV in all four brain regions showed no significant difference from the control values.

1.5 *In vivo* metabolite analysis

The R_f value of [^{77}Br]OBDV as a standard on TLC using mobile phase of hexane: ethyl acetate: triethylamine (3:1:0.1, v/v/v) was 0.26 (Figure 10). In the brain samples, a strong spot of R_f value 0.26 ± 0.02 and a very weak trace spot around the starting point were observed on the TLC plate. In the plasma samples, only a highly polar radioactive metabolite around the starting point was seen on the TLC plate.

1.6 Partition coefficient:

The partition coefficient of [^{77}Br]OBDV was 2.93 ± 0.03 . This result indicates that [^{77}Br]OBDV has a reasonable degree of lipid solubility to penetrate the blood–brain barrier.

1.7 *Ex vivo* autoradiography:

The accumulation in VAcHT-rich regions of the rat brain was visualized in the *ex vivo* autoradiography experiment with [^{77}Br]OBDV [Figure 11 (a)]. The distribution of [^{77}Br]OBDV with high accumulation of the radiotracer was revealed in the cerebral cortex, striatum, diagonal band, hippocampus, thalamus and amygdaloidal nucleus. In the cerebellum, the localization of [^{77}Br]OBDV binding was also witnessed in the molecular and granular cell layers, facial nucleus and trigeminal nucleus. With the co-injection of $0.250 \mu\text{mol}$ (+/-)-vesamicol with [^{77}Br]OBDV, no specific accumulation of the radiotracer was observed in any brain regions of rats [Figure 11 (b)].

2. Discussion:

The intracerebral biodistribution pattern of [⁷⁷Br]OBDV (Table 2) revealed maximum accumulation of radioactivity (>0.6 % ID/g) at 2 min post-injection in all the brain regions and confirmed the rapid penetration of [⁷⁷Br]OBDV through BBB. It indicates that [⁷⁷Br]OBDV have suitable lipophilicity to be extracted in the brain.

Initial brain uptake of [⁷⁷Br]OBDV at 2 min post-injection was relatively homogeneous in the brain regions. This homogenous biodistribution is assumed to express the nonspecific binding of [⁷⁷Br]OBDV reflected by cerebral blood flow in the brain. However, the specific brain regional accumulation of [⁷⁷Br]OBDV was revealed 30 min after intravenous injection. The highest radioactivity distribution of [⁷⁷Br]OBDV was observed in the striatum. Moderate to high distribution of radioactivity was also observed in the cortex, cerebellum and the other regions of the brain. This result indicates that [⁷⁷Br]OBDV accumulated throughout the whole brain, which is in accordance with the brain regional accumulation of [¹²⁵I]OIDV (Kozaka et al., 2014).

The initial blood uptake of [⁷⁷Br]OBDV was low (0.14 ± 0.01 & ID/g). The wash out from the blood was quite fast and at 60 min post-injection, the radioactivity in blood was 0.04 ± 0.01 % ID/g. The low blood uptake and fast blood clearance are advantageous for brain imaging.

In the *in vivo* blocking studies, (+/-)-vesamicol (0.250 μmol) showed significant blocking effects on the regional brain distribution of [⁷⁷Br]OBDV, demonstrating that [⁷⁷Br]OBDV binds to vesamicol binding site on VAcHT with high affinity (Figure 8). In contrast, no significant inhibition of the uptake of [⁷⁷Br]OBDV in any brain region was observed with both the (+)-pentazocine (selective σ-1 receptor agonist) or (+)-3-PPP (σ-1 and σ-2 receptor agonist), separately co-injected with [⁷⁷Br]OBDV into the rats. This negligible changes in *in vivo* brain regional uptake of [⁷⁷Br]OBDV, co-injected with 250

μmol of (+)-pentazocine or (+)-3-PPP, confirm that [^{77}Br]OBDV does not significantly bind to σ -1 and σ -2 receptors like most vesamicol analogues do, presumably because the *o*-Br group of [^{77}Br]OBDV prevents binding to σ -1 and σ -2 receptors but not VAcHT.

The presence of radiolabeled metabolites in the brain can have a negative influence on the imaging of VAcHT; therefore, we examined the *in vivo* metabolism of [^{77}Br]OBDV in the blood and brain of SD rats (60 min post-injection) using TLC (Figure 9). Most of the radioactivity in the brain was unchanged with [^{77}Br]OBDV, but only a polar metabolite of [^{77}Br]OBDV was observed in the blood. This result indicates that the distribution of radioactivity in the rat brain at 60 min post-injection results only from [^{77}Br]OBDV. The increased uptake of radioactivity in the pancreas or small intestine, even at 60 min post-injection, was assumed to be due to metabolites of [^{77}Br]OBDV.

As shown on the autoradiograms [Figure 10(A)], [^{77}Br]OBDV was distributed in VAcHT-rich regions of the rat brain, including the cerebral cortex, striatum, diagonal band, hippocampus, thalamus, amygdaloidal nucleus, cerebellum, and nuclei of cranial nerves at 30 min post-injection. Regions of interests (ROIs) were placed over several brain regions with a reference brain atlas. Relative radioactivity concentration (RRC) on the brain regions were measured by using an image analysis software (Multi Gauge version 3, Fujifilm) and expressed as photostimulated luminescence (PSL)/area (mm^2) (Table 3). The distribution pattern of radioactivity was heterogeneous, with the highest level in the striatum. The brain regional distribution results of table 2 almost accord with the RRC of the brain regions of table 3.

The regional accumulation revealed from the autoradiograms of [^{77}Br]OBDV were in accordance with the distribution of VAcHT-rich brain regions such as pre-synaptic cholinergic nerve terminals, as shown in immunohistochemical studies (Ichikawa T et al.,

1997) as well as the brain regional accumulation of [¹²⁵I]OIDV (Kozaka et al., 2014). VAcHT exists in the pre-synapse of cholinergic nerve systems and mediates the transportation of acetylcholine (ACh) to the cholinergic synaptic vesicles. VAcHT-rich presynaptic cholinergic nerve terminals were thought to be widely distributed in various brain regions, including the cerebral cortex, striatum, diagonal band, hippocampus, thalamus, amygdaloid nucleus, cerebellum, and nuclei of cranial nerves, which was also revealed in the autoradiographic study of [⁷⁷Br]OBDV. As a result the accumulation of [⁷⁷Br]OBDV was observed throughout the whole brain regions in *ex vivo* autoradiography.

Hence, OBDV, with a framework of DV and a halogen atom (-Br) at the ortho-position of the 4-phenylpiperidine moiety, has the potential to be a promising PET VAcHT imaging probe with the characteristics of high lipophilicity, low affinity for σ -1 and σ -2 receptors and high selectivity for VAcHT, in comparison with (+/-)-vesamicol and/or other vesamicol derivatives.

3 Experimental

3.1 Radiosynthesis and purification of [⁷⁷Br]OBDV:

[⁷⁷Br]OBDV was radiosynthesized by the tin-bromine exchange reaction from the trimethylstannyl precursor, OTDV, with [⁷⁷Br]Br⁻, HCl and chloramine-T (Figure 7). [⁷⁷Br]Br⁻ was produced in the cyclotron facility of the biomedical imaging research center of Fukui University. Briefly, [⁷⁷Br]Br⁻, (18.5 MBq/5~10 μ L in EtOH) was added to a reaction vial containing OTDV (21.2 mM in EtOH, 50 μ L), followed by the addition of 0.1 M HCl (50 μ L) and aq. chloramine T (23.7 mM in H₂O, 40 μ L). The reaction mixture was shaken for 5 min at room temperature and then incubated at 77°C for 30 min. The reaction mixture was quenched by the addition of Na₂S₂O₅ (15.8 mM in H₂O, 20 μ L) and 6 M NH₃ (100 μ L). The resultant mixture was passed through a Sep-Pack C-18 light column to remove unreacted water-soluble by products. After washing the Sep-Pack C-18

light column with an additional 15 mL H₂O, the trapped [⁷⁷Br]OBDV in the column was eluted with 5 mL EtOH. The eluent was then concentrated by heating under N₂.

During the purification of [⁷⁷Br]OBDV with HPLC, no UV peak of OBDV was detected because the concentration of OBDV was less than the detection limit. Then, the detection limit of OBDV was estimated using the different concentrations (10³ μM ~ 10⁻⁵ μM) of reference OBDV. The specific activity (SA) of [⁷⁷Br]OBDV was calculated from the activity of the pure [⁷⁷Br]OBDV and the mass of OBDV, assessed from the detection limit of OBDV (1×10⁻¹ μM).

3.2 *In vivo* biodistribution

Animal experiments were carried out in compliance with the *Guidelines for the Care and Use of Laboratory Animals* at the Takara-machi Campus of Kanazawa University. For the biodistribution studies, 0.129 MBq (317.7 fmol) of [⁷⁷Br]OBDV in 400 μL of 5% ethanol/saline solution (v/v) was injected intravenously via the tail vein into SD rats (8 weeks, male, 250-300 g, n = 4 in each group). At 2, 30 and 60 min post-injection, the rats were sacrificed by decapitation under anesthesia with diethyl ether and blood samples were collected. The brain was removed and immediately placed on ice and dissected into segments consisting of four parts (cerebral cortex, striatum, cerebellum, and the rest). The blood, urine, brain regions, and the organs of interest (heart, lung, liver, spleen, pancreas, stomach, small intestine, kidney and bladder) were harvested and weighed. The radioactivity of each part was measured with an auto well gamma system (AccuFLEX γ7010; Aloka). Data were calculated as the percent of injected dose per gram of tissue (% ID/g).

3.3 *In vivo* blocking studies

Receptor blocking experiments were performed to evaluate the specific uptake of [⁷⁷Br]OBDV. SD rats (8 weeks, male, 250-300 g, n = 4 in each group) were randomly

divided into four groups. The rats were injected with 0.111 MBq (273.4 fmol) of [⁷⁷Br]OBDV in 400 μL of 5% ethanol/saline solution (v/v) intravenously via the tail vein with 0.250 μmol (+/-)-vesamicol, 0.250 μmol (+)-3-(3-hydroxyphenyl)-*N*-propylpiperidine, [(+)-3-PPP], 0.250 μmol (+)-pentazocine, and none as a control. At 30 min post-injection, the rats were sacrificed by decapitation under anesthesia with diethyl ether and blood samples were collected. The brain was removed and immediately placed on ice and dissected into segments consisting of four parts (cerebral cortex, striatum, cerebellum, and the rest). The four dissected brain parts were collected and weighed. The radioactivity of each part was measured with an auto well gamma system (AccuFLEX γ7010; Aloka). Analyses of the data from the blocking studies were performed using a one-way ANOVA followed by a Tukey's multiple comparison test (GraphPad Prism Version 4 software). Differences were considered significant when $P < 0.05$.

3.4 *In vivo* metabolite analysis

In vivo metabolite analysis with [⁷⁷Br]OBDV was performed by autoradiographic analysis of thin layer chromatography (TLC). The SD rats (8 weeks, male, 250-300 g, n = 3) received intravenous injection of 0.400 MBq (985.2 fmol) of [⁷⁷Br]OBDV in 400 μL of 5% ethanol/saline solution (v/v) via the tail vein. At 60 min post-injection, the rats were sacrificed by decapitation under anesthesia with diethyl ether and blood samples were collected in a heparin-coated tube. The brain was removed, immediately placed on ice and the brain segments were harvested without the cerebellum. The blood corpuscles were separated by centrifugation at 15000 rpm for 15 min at 4°C. The resulting plasma (300 μL) was separated from the involved macromolecules (>10000 molecular weight) by ultrafiltration. The resulting filtrate was analyzed by TLC using mobile phase of hexane: ethyl acetate: triethylamine (3:1:0.1, v/v/v). The brain tissue was homogenized for 1 min with an ultrasonic homogenizer in acetonitrile and H₂O (2:1). The brain homogenate

suspensions were centrifuged at $20000 \times g$ for 20 min at 4°C . The supernatant was collected and separated from the involved macromolecules (>10000 molecular weight) by ultrafiltration. The resulting filtrate was analyzed by TLC using mobile phase of hexane: ethyl acetate: triethylamine (3:1:0.1, v/v/v). The TLC plates were then exposed to an imaging plate (BAS-IP SR 2025; Fujifilm) for 5 days (120 hrs), after which the plates were scanned by a BAS-5000 phosphoimager (Fujifilm).

3.5 Determination of partition coefficient:

The partition coefficient ($\log P_{o/w}$) of [^{77}Br]OBDV was determined by the standard method using *n*-octanol and 0.1 M phosphate buffer (pH = 7.4). Briefly, [^{77}Br]OBDV was mixed with *n*-octanol (15 mL) and 0.1 M phosphate buffer (15 mL), in each (n) 50 mL centrifuge tube (where, n = 4). Then the mixtures were vortexed for 5 min, followed by centrifugation of the mixture at $1000 \times g$ for 10 min. After centrifugation, 1 mL *n*-octanol and 1 mL phosphate buffer were separately transferred to the polyethylene tube from each centrifuge tube in quadruplicate. The radioactivity of each tube was measured with an auto well gamma system (AccuFLEX γ 7010; Aloka). The partition coefficient was calculated with the formula: $\log P_{o/w} = \log_{10} C_o/C_w$ (radioactivity in *n*-octanol layer/radioactivity in aqueous layer).

3.6 *Ex vivo* autoradiography

In *ex vivo* autoradiography, 1.00-1.58 MBq (2.46-3.89 pmol) of [^{77}Br]OBDV in 400 μL of 5% ethanol/saline solution (v/v) was injected intravenously into SD rats (8 weeks, male, 250-300 g, n = 3) via the tail vein with 0.250 μmol (+/-)-vesamicol, and none as a control. At 30 min post-injection, the rats were sacrificed by decapitation under anesthesia with diethyl ether and blood samples were collected. The whole brain was harvested and immediately frozen in Tissue-Tek O.C.T. Compound (Sakura Finetek) at -78°C . The frozen brain was cut into 20- μm -thick horizontal slices at -20°C using a

cryostat microtome (HM 525 Cryostat; Thermo Scientific) and mounted on glass slides. The slices were then exposed to an imaging plate (BAS-IP SR 2025; Fujifilm) for 2 days, after which the plates were scanned by a BAS-5000 phosphoimager (Fujifilm).

Conclusion:

In vitro HAcHT [³H]HC-3 competitive binding assay revealed no affinity of THA, DMTA, PTAA and MKC-231 towards HAcHT. In efforts for the development of PET VAcHT imaging probe, [⁷⁷Br]OBDV was radiosynthesized with radiochemical purity of greater than 99%, and the radiochemical yield was 52.3 ~ 65.8%. The specific activity of [⁷⁷Br]OBDV was found to be 322 ~ 406 GBq/μmol. *In vivo*, [⁷⁷Br]OBDV appeared to bind selectively to VAcHT with high affinity. *Ex vivo* autoradiography revealed that [⁷⁷Br]OBDV accumulated in the corresponding VAcHT-rich regions in the rat brain. Hence, it can be concluded that [⁷⁶Br]OBDV has the potential to be a prospective VAcHT PET ligand for the early diagnosis of AD.

References:

- Ichikawa T, Ajiki K, Matsuura J, Misawa H. 1997. Localization of two cholinergic markers, choline acetyltransferase and vesicular acetylcholine transporter in the central nervous system of the rat: In situ hybridization histochemistry and immunohistochemistry. *J Chem Neuroanatomy* 13:23–39.
- Kozaka T, Uno I, Kitamura Y, Miwa D, Ogawa K, Shiba K. 2012. Syntheses and in vitro evaluation of decalinvesamicol analogues as potential imaging probes for vesicular acetylcholine transporter. *Bioorganic & medicinal chemistry* 20(16):4936-4941.
- Kozaka T, Uno I, Kitamura Y, Miwa D, Azim MA, Ogawa K, Shiba K. 2014. Regional brain imaging of vesicular acetylcholine transporter (VACHT) using *o*-[¹²⁵I]iodo-*trans*-decalinvesamicol as a new potential imaging probe. *Synapse* 68(3): 107-113.
- Quirion R. 1987. Characterization and autoradiographic distribution of HC-3 high affinity choline uptake sites in mammalian brain. *Synapse* 1: 293-303.
- Sandberg K, Coyle JT. 1985. Characterization of [³H]HC-3 binding associated with Neuronal choline uptake sites in rat membranes. *Brain research* 348: 321-330.

Table 1. *In vitro* binding assay of vesamicol analogues (Kozaka T et al., 2012).

Entry	Compounds	Ki (nM)		
		VAcHT	σ -1	σ -2
1	OIDV	20.5 ± 5.6	241.8 ± 98.9	118.8 ± 57.0
2	OBDV	13.8 ± 1.2	150.7 ± 62.9	137.5 ± 97.4
3	DV	13.6 ± 8.8	74.1 ± 39.9	68.3 ± 25.5
4	vesamicol	33.9 ± 18.1	22.1 ± 3.6	86.7 ± 35.7
5	DTG	-	131.1 ± 39.2	31.7 ± 3.6
6	pentazocine	-	12.1 ± 5.0	1,880.8 ± 953.9
7	haloperidol	-	3.5 ± 0.8	51.6 ± 14.6

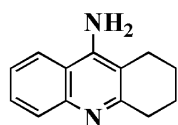
Table 2: Biodistribution of [⁷⁷Br]OBDV in rats after intravenous injection of the tracer^a

Tissue	Post injection time		
	2 min	30 min	60 min
Blood	0.14 ± 0.01	0.11 ± 0.12	0.04 ± 0.01
Heart	2.19 ± 0.52	0.39 ± 0.03	0.27 ± 0.03
Lung	5.57 ± 0.72	1.54 ± 0.24	1.23 ± 0.14
Pancrease	2.10 ± 0.55	2.52 ± 0.98	2.98 ± 0.33
Spleen	0.89 ± 0.34	1.35 ± 0.25	1.02 ± 0.23
Kidney	2.90 ± 0.36	2.18 ± 0.27	1.68 ± 0.52
Bladder	0.15 ± 0.04	0.19 ± 0.04	0.20 ± 0.03
Urine	0.04 ± 0.04	0.25 ± 0.02	0.32 ± 0.24
Small intestine	0.93 ± 0.14	1.24 ± 0.44	1.69 ± 0.26
Stomach	0.26 ± 0.19	0.32 ± 0.28	0.22 ± 0.14
Liver	1.04 ± 0.12	1.79 ± 0.05	1.62 ± 0.04
Cerebral cortex	0.64 ± 0.06	0.52 ± 0.11	0.50 ± 0.05
Striatum	0.62 ± 0.08	0.59 ± 0.05	0.53 ± 0.09
Cerebellum	0.61 ± 0.09	0.56 ± 0.04	0.45 ± 0.05
Others	0.61 ± 0.07	0.58 ± 0.05	0.50 ± 0.05

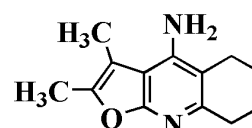
^aRadioactivities are expressed as % injected dose per gram tissue (% ID/g). The values are the mean ± standard deviation (SD) of four rats (n = 4) at each time point.

Table 3: RRC of [⁷⁷Br]OBDV on the brain regions.

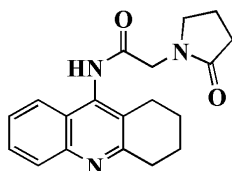
Brain Regions	Cerebral Cortex	Striatum		Diagonal band	Hippocampus	Cerebellum	Posterolateral cortical Amygdaloidal nucleus
		Lateral	Internal				
RRC (PSL/mm ²)	56.6 ± 1.5	61.8 ± 1.4	59.8 ± 1.2	60.5 ± 1.7	53.5 ± 1.5	50.4 ± 0.8	51.5 ± 1.2



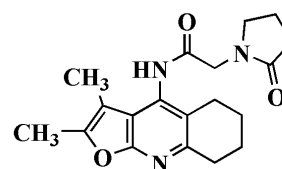
1,2,3,4-Tetrahydro-acridin-9-yl
Amine (Tacirine)



2,3-dimethyl-5,6,7,8-tetrahydrofuro
[2,3-b]quinolin-4-amine (DMTA)

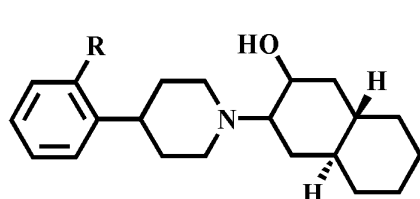


2-(2-Oxo-pyrrolidin-1-yl)-N-(1,2,3,4-tetrahydro-acridin-9-yl)-acetamide (PTAA).



2-(2-Oxo-pyrrolidine-1-yl)-N-(2,3-dimethyl-5,6,7,8-tetrahydrofuro [2,3-b]quinolin-4-yl) acetoamide (MKC-231).

Figure 1: Chemical Structures of Tacirine, DMTA, PTAA and MKC-231.



OBDV: R = Br
OTDV: R = SnMe₃
OIDV: R = I

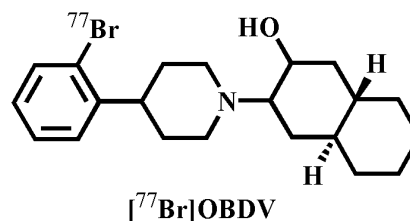


Figure 2: Structure of OBDV, OTDV, OIDV and [⁷⁷Br]OBDV

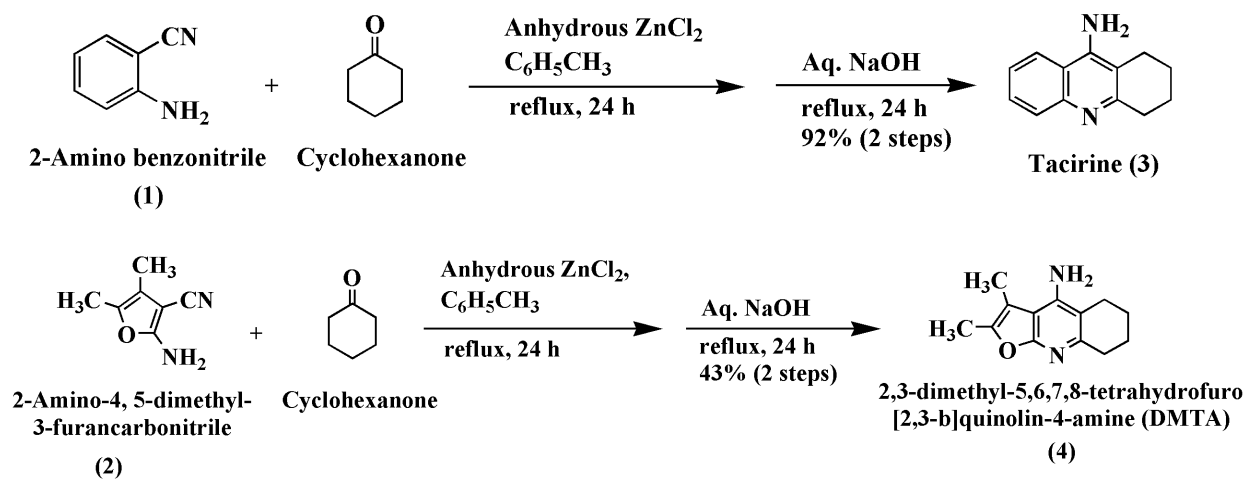


Figure 3: Scheme for the syntheses of tacirine and DMTA.

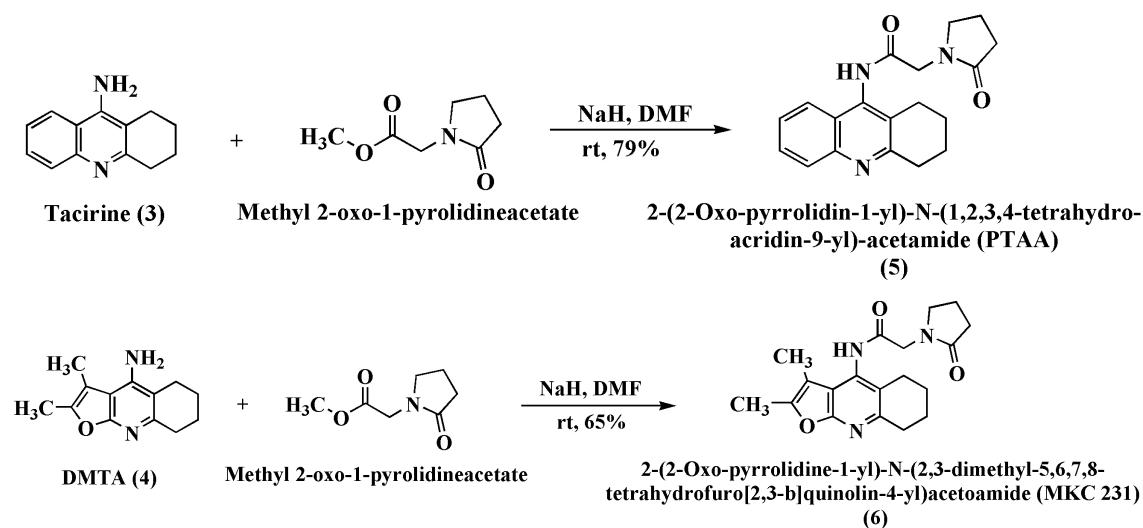


Figure 4: Scheme for the syntheses of PTAA and MKC-231.

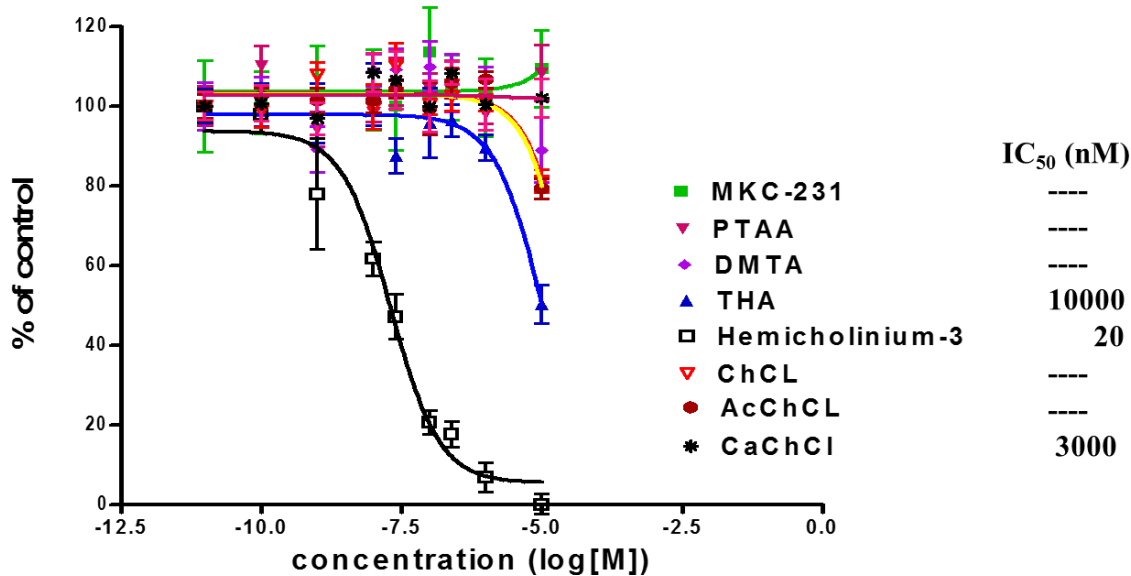


Figure 5: HACHT [³H]Hemicholinium-3 binding assay

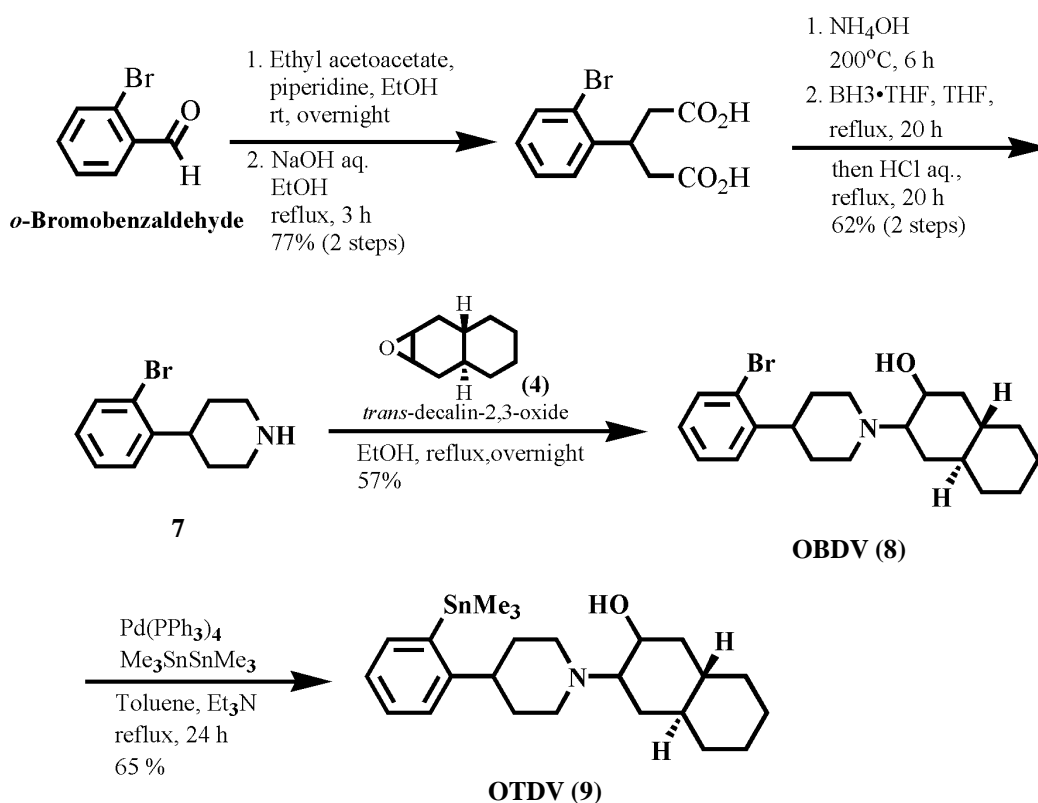


Figure 6: Synthesis scheme of OBDV and OTDV

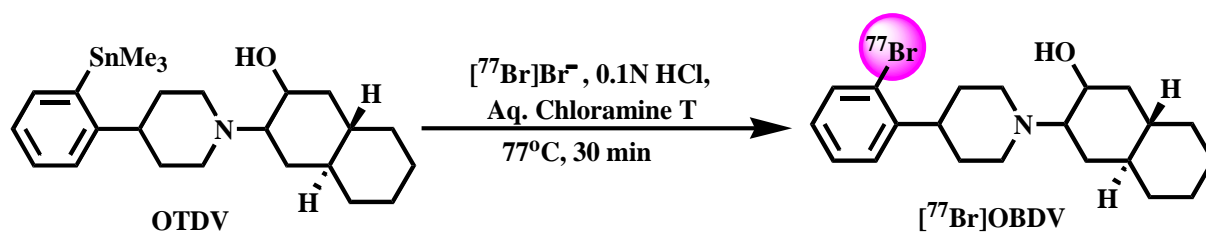


Figure 7: Radiosynthesis of $[\text{}^{77}\text{Br}]\text{OBDV}$.

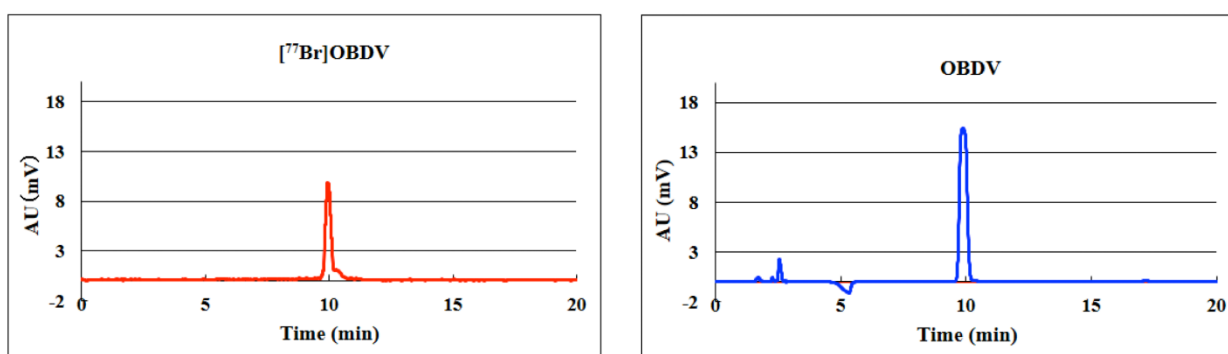


Figure 8 : HPLC charts for the retention time of $[\text{}^{77}\text{Br}]\text{OBDV}$ and reference OBDV.

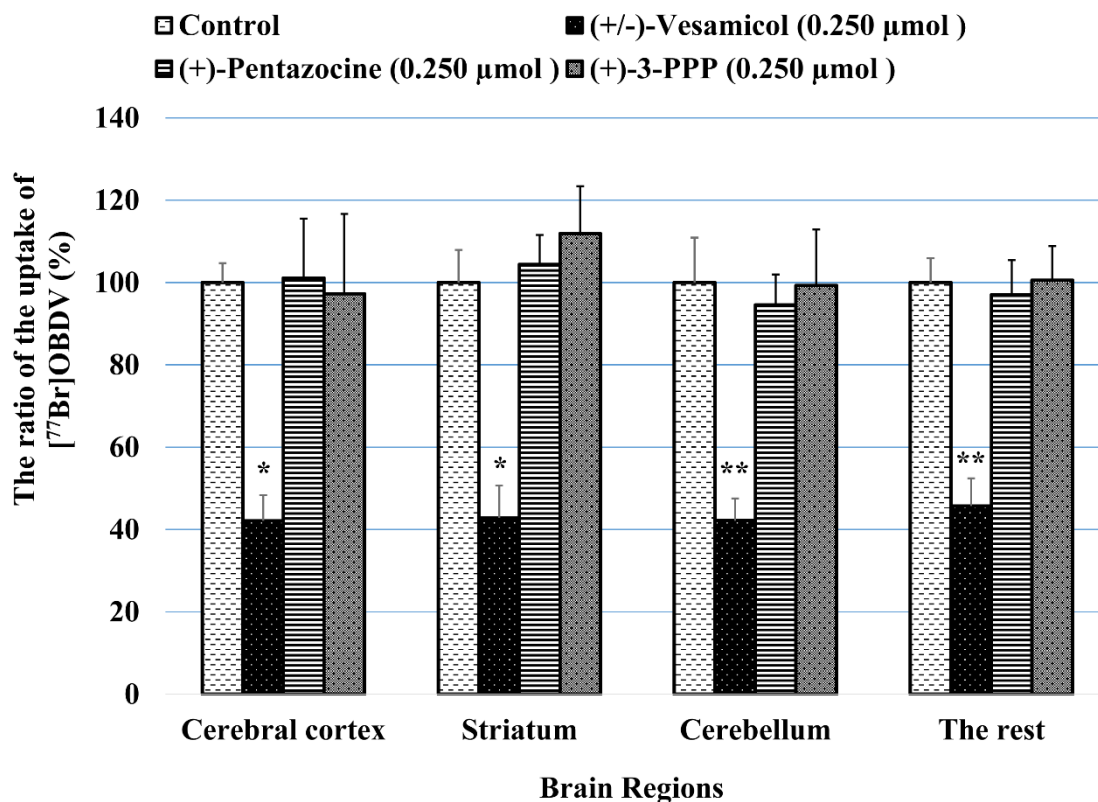


Figure 9: The effect of inhibitors on the uptake of [⁷⁷Br]OBDV. The vertical axis shows the mean radioactivity rate in the brain regions (cerebral cortex, striatum, cerebellum, and the rest) of each group co-injected with (±)-vesamicol (0.250 μmol) or (+)-pentazocine (0.250 μmol) or (+)-3-PPP (0.250 μmol), estimating the control ([⁷⁷Br]OBDV only) as 100%. The stars (*) in the figure indicate the significant difference between the uptake of [⁷⁷Br]OBDV co-injected with (+/-)-vesamicol (0.250 μmol) and none as control in all the brain regions. A one-way ANOVA followed by a Tukey’s multiple comparison test was performed by GraphPad Prism Version 4 software, compared with the control. Here, *P <0.01 and **P <0.001.

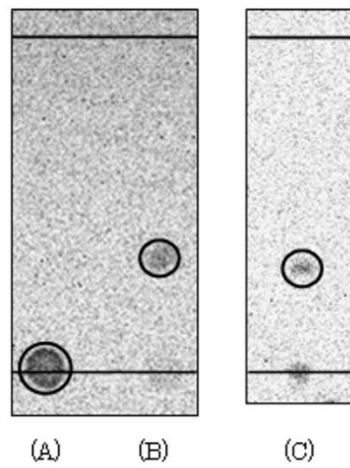


Figure 10: In vivo metabolite analysis of [^{77}Br]OBDV in the rat brain 60 minutes after intravenous injection. Here, (A) & (B) indicate TLC analysis of plasma and brain samples, respectively, and (C) indicates TLC analysis with the control ([^{77}Br]OBDV).

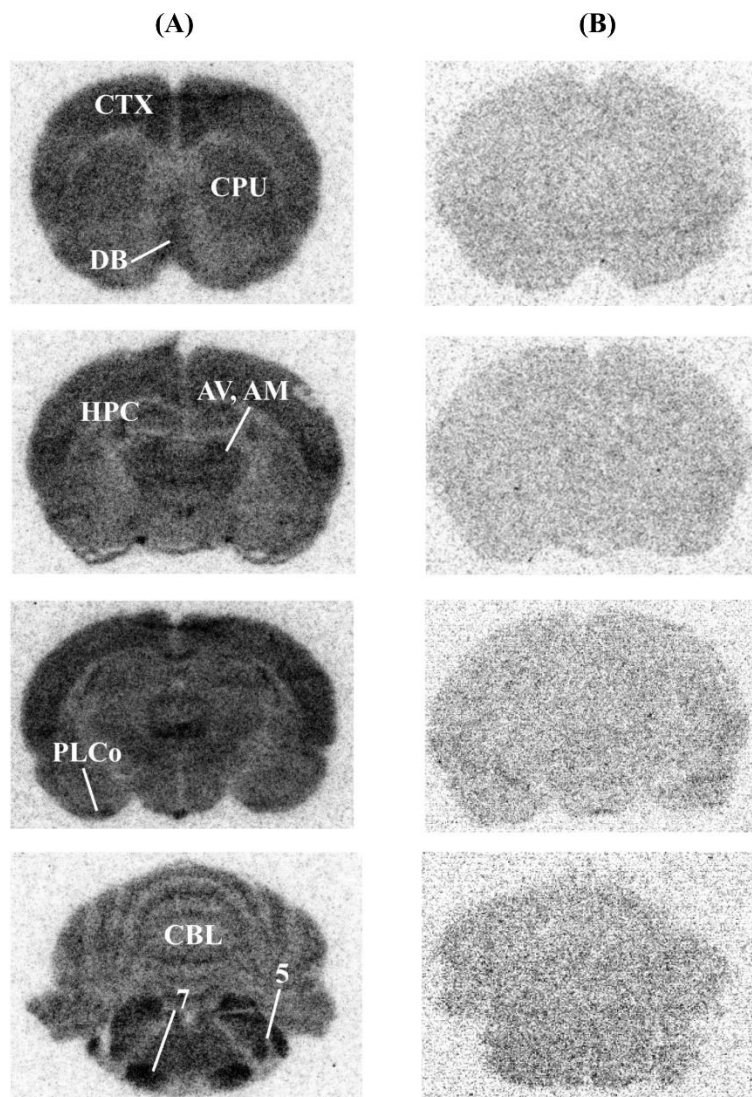


Figure 11: *Ex vivo* autoradiographic distribution of [⁷⁷Br]OBDV in the rat brain at 30 min post-injection (A) with the control ([⁷⁷Br]OBDV only); (B) co-injection of 0.250 μmol (+/-)-vesamicol with [⁷⁷Br]OBDV in the rat brain as an inhibitor. Abbreviations: AM, anteromedial thalamus; AV, anteroventral thalamus; CBL, cerebellum; CPU, striatum; CTX, cerebral cortex; DB, diagonal band; HPC, hippocampus; PLCo, posterolateral cortical amygdaloidal nucleus; 5, trigeminal nucleus; 7, facial nucleus.

学位論文審査報告書 (甲)

1. 学位論文題目 (外国語の場合は和訳を付けること。)

Development of Novel Radiotracer for Imaging High Affinity Choline Transporter and Vesicular and Acetyl Choline Transporter

新規放射性コリン作動性神経系トランスポーターイメージング剤の開発に関する研究

2. 論文提出者 (1) 所属 生命科学 専攻

(2) 氏名 Azim Mohammad Anwar-UL (アジム モハムド アンワル ウル)

3. 審査結果の要旨 (600~650 字)

本学位論文はアルツハイマー病の重症度ならびに治療効果判定の客観的診断法の開発を目指して、アルツハイマー病の症状と関連の深いコリン作動性神経系の前シナプスに存在するコリントランスポーター(ChT)とアセチルコチントランスポーター(VAChT)に着目し、PET 用 ChT 及び VAChT 分子イメージング剤の開発を検討したものである。ChT の研究においては、ChT に高い親和性を有する hemicholinium-3(HC-3)は水溶性であり BBB を通過しないため分子イメージング剤としては不向きである。そのため、ChT 活性を増強させる化合物群を合成し、*in vitro*での ChT 親和性を調べたが、ChT 高親和性化合物の合成は不成功に終わった。しかし、VAChT の研究においては、VAChT に対して親和性有する vesamicol 類縁体から o-bromo-trans-decalinevesamicol (OBDV)を設計し合成に成功した。In vitro 実験の結果、OBDV は VAChT に対して高い親和性を有するだけでなく、シグマ受容体への親和性も低く、選択性にも優れていることがわかった。そこで、放射性臭素核種 (^{77}Br)での標識を検討し、高い放射化学的収率かつ高比放射能で ^{77}Br 標識体を得ることに施行した。さらに、新規 VAChT 分子イメージング剤としての有用性を *in vivo*動物実験により評価した。その結果、*in vivo* 阻害実験や *ex vivo*オートラジオグラフィ実験等において、脳内では ^{77}Br OBDV が VAChT に選択的に集積することを確認した。また、 ^{77}Br OBDVは脳内では代謝を受けずに ^{77}Br OBDVのまま集積していることがわかった。以上のことから、放射性臭素核種で標識した OBDV が PET 用の新規 VAChT 分子イメージング剤として有望であることを明らかにした。この成果は、学位授与に値する研究と評価できる。

4. 審査結果 (1) 判定 (いずれかに○印) 合格 ・ 不合格

(2) 授与学位 博士 (薬学)